19th Brazilian Congress of Thermal Sciences and Engineering
November 06th-10th, 2022, Bento Gonçalves - RS - Brazil

ENC-2022-0104
THERMODYNAMIC MODELLING OF ROTATING DETONATION ENGINES CYCLES

Robson Eduardo dos Anjos Schneider
Universidade Federal do Rio Grande do Sul
Rua Sarmento Leite, 425, Centro Histórico, Porto Alegre, Brasil
robson.schneider@ufrgs.br
Cesar Celis
Pontificia Universidad Católica del Perú
Av. Universitaria 1801, San Miguel, Lima 32, Lima, Peru
ccelis@pucp.edu.pe
Andrés Armando Mendiburu Zevallos
Universidade Federal do Rio Grande do Sul
Rua Sarmento Leite, 425, Centro Histórico, Porto Alegre, Brasil
andresmendiburu@ufrgs.br

Abstract. *This work aims to perform a thermodynamic comparison of the thermal efficiency of gas turbines operating with a combustion chamber and a detonation chamber, using methane, ethanol and mixtures of ethanol and hydrogen and methane and hydrogen as fuels. Based on the study of combustion reactions in the context of equilibrium thermodynamics, a computational model was developed in order to study the combustion and detonations processes. The composition of the gases is determined by the minimization of the Gibbs free energy and the temperature, pressure and speed of detonation are determined by the Chapman-Jouguet theory. The results obtained showed that the detonation thermodynamic cycle had a higher compressor work, turbine work, turbine net work output and thermal efficiency than the constant-pressure combustion cycle for all fuels considered. The maximum thermal efficiency obtained with the detonation cycle was 48.88%, which is a 42.91% improvement over the maximum thermal efficiency obtained with the constant-pressure combustion cycle.*

Keywords: *Rotating detonation engines, thermal efficiency, thermodynamic model*

1. INTRODUCTION

A rotating detonation engine (RDE) is a type of engine where the reactants are fed into the combustor and the detonation waves travels around the circumference of the combustor with supersonic speed, performing work through pressure gain combustion. Rotating detonation engines can be applied to power-generating devices, such as a gas-turbine, or to give propulsion to vehicles, like aircrafts (Wolański, 2013). Studies have claimed that, with a rotating detonation engine, it is possible to achieve a decrease of 9% in fuel consumption compared to traditional gas-turbine engines, an increase of up to 15% in the total pressure in the combustor due to detonation, an increase of 5% in thermal efficiency (considering a gas-turbine setting), an increase in thermal efficiency of 4.6% (with just the combustor) and up to 14% increase in power plant efficiency over conventional J class turbines (Anand and Gutmark, 2019).

Zheng *et al*. (2018) performed a numerical investigation into the pressure gain performance of continuously rotating detonation (CRD) combustors, using methane–air as a reactive mixture and under the operating conditions of a micro gas turbine. Numerical results showed that the pressure gain characteristics of the CRD combustors was associated with the corresponding change in Gibbs free energy. Compared to approximate constant pressure-based combustors, CRD combustors with lower Gibbs free energy loss could offer a significant advantage in terms of pressure ratio. Sousa *et al.* (2017) carried out a Thermodynamic analysis of a gas turbine engine with a rotating detonation combustor and, by comparison, concluded that, the gas turbine equipped with a rotating detonation combustor versus the conventional deflagration combustor demonstrated the potential benefits of the pressure gain combustion at low pressure ratios. The efficiency gain is above 5% at low pressure ratios, although the gain is less prevalent at high compression ratios. Folusiak *et al*. (2020) showed that, for low pressure ratios between the inlet and outlet of the chamber, a stable propagation of wave is possible, although significant losses can occur because of strong series of shockwaves observed at the expansion section of the RDE. it is concluded that the better mode of operation of the RDE combustion chamber is supersonic mode.

Such attributes make the rotating detonation engine an attractive choice to improve the efficiency of gas-turbines in general. On the other hand, the high energy density and the near-stoichiometric operation of the RDE makes the device's thermodynamic analysis complex. Equivalence ratios close to the stoichiometric proportion also results in exhaustion products of high temperature that need to be diluted with efficiency. The high variation of pressure on a rotating detonation engine can cause structural failure on the components of the engine, since they work near the mechanical limit, and, also, it can have consequences on the turbine's efficiency, as shock waves and flow separation may be prejudicial. Such factors, among others, means that rotating detonation engines are still in an experimental stage of development and are not mass-produced.

Although many beneficial conclusions have been achieved through the exploratory studies of rotating detonation engines, Xie *et al*. (2020) argue that the flow and physicochemical processes involved in rotating detonation technology are quite complex, and the mechanism of rotating detonation combustion still needs further studying, such as the formation and self-sustaining mechanism of the rotating detonation wave, the generation mechanism of the instable detonation wave, and the mechanism controlling instability with high efficiency.

Thus, this work aims to perform a thermodynamic comparison of the thermal efficiency of gas turbines operating with a combustion chamber and a detonation chamber, considering different fuels, such as methane, ethanol and hydrogen. For that, a thermodynamic model was developed, where the composition of the gases is determined by the minimization of the Gibbs free energy and the temperature, pressure and speed of detonation are determined by the Chapman-Jouguet theory. The present work explores the influence of parameters such as compression ratio, fuel composition and equivalence ratio in the thermal efficiency generated.

2. METHODOLOGY

The constant-pressure combustion and detonation cycle models were developed based in thermodynamics fundamentals (Moran *et al.*, 2018), equilibrium combustion theory (Carvalho Jr. *et al.*, 2018), and Chapman-Jouguet theory for detonations (Lee, 2005 and Kuo, 2008). The nozzle was modeled using the theory presented by Shapiro (1953) and its operational condition is that of steady-state.

The constant-pressure combustion cycle and the detonation cycle were compared through a range of compression ratios (*rc*) that span the interval between 4 and 40. The gas turbine operating with a conventional combustion chamber was modelled considering a constant-pressure combustion thermodynamic cycle, as shown on Figure 1.

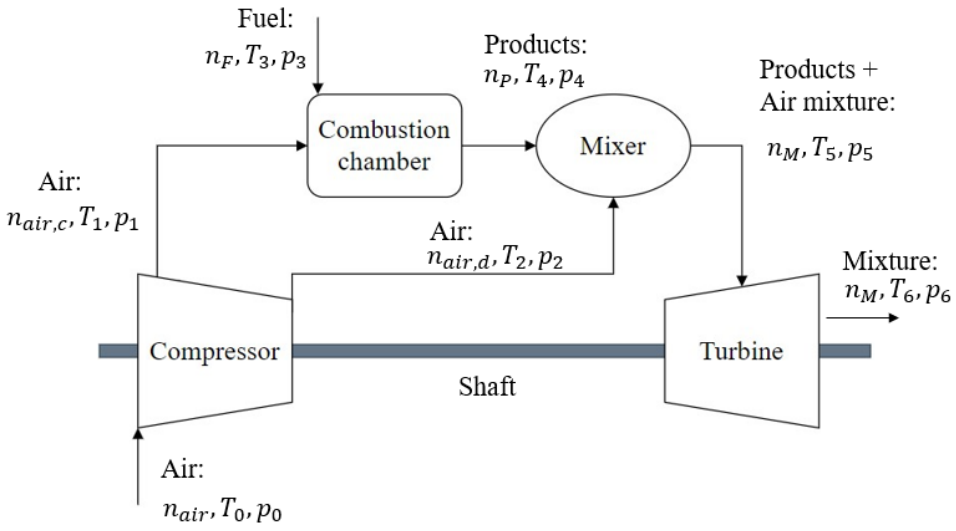

Figure 1. Constant-pressure combustion thermodynamic cycle considered in the simulations.

Air enters the compressor at an initial temperature of T_0 and initial pressure of p_0. The number of mols of air admitted is referred as n_{air}. The compressed air enters the combustion chamber at temperature T_1, pressure p_1 and $n_{air,c}$ number of moles. The combustion chamber is fed with four different fuels: methane (CH_4), ethanol (C_2H_5OH), a blend of $75\%\ CH_4 + 25\%\ H_2$ and a blend of $50\%\ CH_4 + 50\%\ H_2$. Combustion occurs on the combustion chamber at constant-pressure and it is an adiabatic process. No work is performed, nor changes in kinetic and potential energy happens. Also, it is considered that the combustion is stoichiometric. On the mixer, the mixing between the combustion gases and diluted air coming from compressor will take place. The mixing process is also adiabatic and occurs at constant-pressure. On the turbine, the mixture of gases coming from the mixer will be expanded and work will be performed.

The gas turbine operating with a detonation chamber was modelled considering a detonation thermodynamic cycle, as shown on Figure **2**.

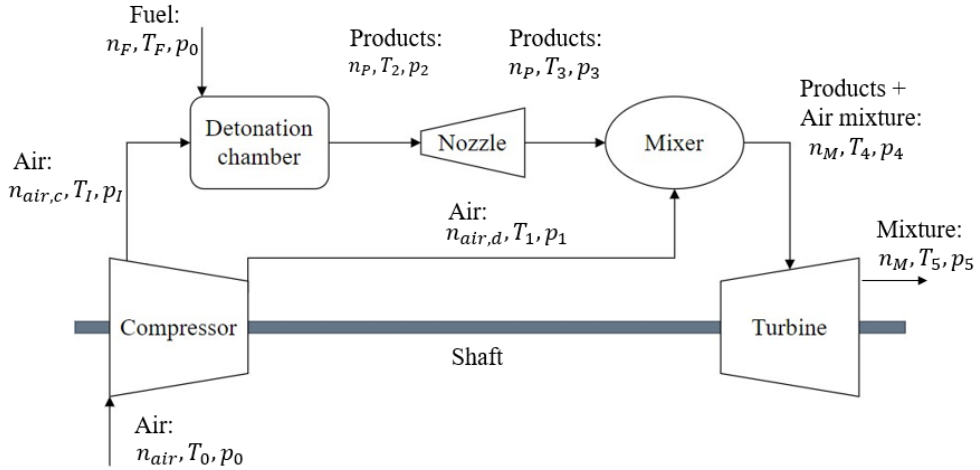

Figure 2. Detonation thermodynamic cycle considered in the simulations.

In the detonation cycle, air is extracted from the compressor at an intermediate pressure p_I. The ratio between p_I and the outlet pressure of the compressor (p_1) is called pressure fraction. Two different pressure fractions were considered: 0,1 and 1. Also, the cycle displayed in Figure **2** features a nozzle, which is applied to cool the temperature of the gases exhausted from the detonation chamber. The reference for initial temperature and initial pressure are equal to 298,15 K and 100 kPa, respectively, according to IUPAC (1982). The global combustion reaction is given by Eq. (1).

$$C_{x_C}H_{x_H}O_{x_O}N_{x_N} + \frac{\nu_{air}^s}{\phi}(O_2 + 3{,}76N_2) \rightarrow n_{CO_2}CO_2 + n_{CO}CO + n_{H_2O}H_2O + n_{H_2}H_2 + n_{O_2}O_2 + n_{NO}NO + n_{N_2}N_2 \quad (1)$$

In Eq. (1), n_i refers to the number of mols of chemical species i and ν_{air}^s is the reaction's air coefficient. Since the combustion is stoichiometric, the equivalence ratio ϕ is equal to unity. Equation (2) shows the real work done by the compressor (W_C), in J.

$$W_C = n_{air}(\bar{h}_I - \bar{h}_o) + n_{air,d}(\bar{h}_1 - \bar{h}_I) \quad (2)$$

In Eq. (2), n_{air} refers to the quantity of air that enters the compressor and $n_{air,d}$ refers to the diluted air that goes to the mixer. Both are expressed in unit of mol. $\bar{h}_o$, $\bar{h}_I$ and $\bar{h}_1$ are the molar enthalpies of air in initial, intermediate and final states of the compression stage, respectively. The three aforementioned enthalpies are expressed in J/mol. In the constant-pressure combustion cycle, there is no pressure fraction (i.e., there is no intermediate stage), so, in that case, $\bar{h}_I = \bar{h}_1$. All the thermodynamical properties are determined computationally utilizing the NASA-Glenn polynomials and coefficients as reference (Gordon *et al.*, 2002). The air at the inlet of the compressor is composed of 21% of O_2 and 79% of N_2. The quantity of air that takes part in the reaction, $n_{air,c}$, is given by Eq. (3).

$$n_{air,c} = 4{,}76 \cdot \nu_{air}^s \quad (3)$$

The compression process features an isentropic efficiency $\eta_{i,c}$ considered equal to 0,85. Equation (4) shows the relation between the real compressor work and the isentropic efficiency, while Eq. (5) gives the relation between the isentropic efficiency, the enthalpy of air in the initial state, $\bar{h}_o$, the real molar enthalpy of air in the intermediate state, $\bar{h}_I$, and the isentropic molar enthalpy in the intermediate state of the air, $\bar{h}_{I,s}$.

$$\eta_{i,c} = \frac{W_{C,ideal}}{W_{C,real}} \quad (4)$$

$$\eta_{i,c} = \frac{\bar{h}_{I,s} - \bar{h}_o}{\bar{h}_I - \bar{h}_o} \quad (5)$$

Equation (6) gives the relation between the isentropic efficiency, the enthalpy of air in the initial state, $\bar{h}_o$, the real molar enthalpy of air in the final state of the compression process, $\bar{h}_1$, and the isentropic molar enthalpy in the final state of the compression process, $\bar{h}_{1,s}$.

$$\eta_{i,c} = \frac{\bar{h}_{1,s} - \bar{h}_o}{\bar{h}_1 - \bar{h}_o} \tag{6}$$

Equation (7) and Equation (8) gives the isentropic molar enthalpies of the intermediate and final stage, respectively. $\bar{S}_o^o$ refers to the molar enthalpy of air in the initial stage and $\bar{R}$ is the universal constant of gases, equal to 8,314 J/mol-K.

$$\bar{S}_{I,s} = \bar{S}_o^o - \bar{R} \cdot \ln\frac{p_I}{p_o} \tag{7}$$

$$\bar{S}_{1,s} = \bar{S}_o^o - \bar{R} \cdot \ln\frac{p_1}{p_o} \tag{8}$$

The sum of the enthalpies of each component species yields the total enthalpies of the products and the reactants. The conservation of energy is achieved because, in the constant-pressure combustion cycle, the total enthalpies of the products and the reactants are equal. The products are found at equilibrium, at an adiabatic flame temperature. In the detonation cycle, the Chapman-Jouguet theory is applied, as shown by Eq. (9), (10) and (11).

$$\dot{m}'' = \rho_P u_P = \rho_R u_R \tag{9}$$

$$p_P + \rho_P u_P^2 = p_R + \rho_R u_R^2 \tag{10}$$

$$h_P + \frac{u_P^2}{2} = h_R + \frac{u_R^2}{2} \tag{11}$$

$\dot{m}$ refers to the mass flux, in $\mathrm{kg/m^2 s}$. ρ_P and ρ_R are the specific masses of the products and the reactants, respectively, in $\mathrm{kg/m^3}$. u_P is the velocity of the products and u_R, the velocity of the reactants. Both are given in units of m/s. h_P and h_R are the specific enthalpies, in J/kg, of the products and the reactants, respectively.

The temperature and pressure reduction provided by the nozzle featured in the detonation cycle (Figure **2**) is yielded by Eqs. (12) and (13). Equation (12) relates, at any given point of the nozzle, the stagnation temperature T_e, along with the temperature T, both in K. Equation (13), in its turn, relates the stagnation pressure p_e with pressure p, both in Pa, at an arbitrary point of the nozzle. k refers to the thermal capacity ratio and M, the Mach number of the combustion products at said arbitrary point.

$$\frac{T_e}{T} = 1 + \frac{k-1}{2}M^2 \tag{12}$$

$$\frac{p_e}{p} = \left(1 + \frac{k-1}{2}M^2\right)^{\frac{k}{k-1}} \tag{13}$$

The products of combustion go through the mixer where they are diluted with the load of compressed air that went through the total compression process in the compressor (i.e., the pressure fraction is equal to 1). The temperature of the mixture of air and combustion products is considered equal to 1500 K. According to De Souza (2014), this temperature is in the range of temperatures where commercial turbines can safely operate. The quantity of air needed to perform the cooling of the gaseous products of combustion to 1500 K is given by Eq. (14).

$$n_{air,d} = \frac{n_P\left(\bar{h}_{P,4} - \bar{h}_{P,3}\right)}{\left(\bar{h}_{air,d,4} - \bar{h}_{air,d,3}\right)} \tag{14}$$

In Eq. (14), n_P refers to the quantity of mols of the combustion products. $\bar{h}_{P,3}$ and $\bar{h}_{P,4}$ are the molar enthalpies of the products in the inlet and outlet of the mixer, respectively. $\bar{h}_{air,d,4}$ and $\bar{h}_{air,d,3}$ are the molar enthalpies of the products in the outlet and inlet of the mixer, respectively. All molar enthalpies are expressed in J/mol. The mixture of diluted air and hot products of combustion are admitted to the turbine, performing an expansion of gases and, therefore, mechanical

work. The work done by turbine, in J, is shown in Eq. (15), where n_M is the molar quantity of the mixture, while $\bar{h}_5$ and $\bar{h}_4$, in J/mol, are the molar enthalpies of the mixture in the outlet and inlet of the turbine, respectively.

$$W_T = n_M(\bar{h}_5 - \bar{h}_4) \tag{15}$$

The isentropic efficiency of the turbine, η_T, is considered equal to 0,9. Equation (16) relates the isentropic efficiency with the isentropic molar enthalpy of the mixture in the outlet of the turbine, $\bar{h}_{5,s}$, the real molar enthalpy of the mixture in the outlet of the turbine, $\bar{h}_5$, and the molar enthalpy in the initial stage, $\bar{h}_4$. All the enthalpies aforementioned are expressed in J/mol.

$$\eta_T = \frac{\bar{h}_4 - \bar{h}_5}{\bar{h}_4 - \bar{h}_{5,s}} \tag{16}$$

The isentropic processes from the inlet to the outlet stage of the turbine are given by Eq. (17). The inlet pressure is equal to the outlet pressure of the compressor, p_1. The outlet pressure is equal to atmospheric pressure, p_0.

$$\bar{S}_{3,s} = \bar{S}_2^o - \bar{R} \cdot \ln\frac{p_1}{p_0} \tag{17}$$

Equation (18) yields the thermal efficiency of the cycle:

$$\eta = \frac{W_T - W_C}{n_F\overline{LHV}} \tag{18}$$

In Eq. (18), W_T and W_C, refers to the real work performed by the turbine and the compressor, respectively. n_F is the molar quantity of the fuel, and it is equal to 1 mol. The molar lower heating value of the fuel, $\overline{LHV}$, is calculated by Eq. (19).

$$\overline{LHV} = \frac{H_R - H_P}{n_F} \tag{19}$$

The work done by the compressor and turbine per unit of mass of fuel is given by Eq. (20) and Eq. (21), respectively, where $m_{F,i}$ represents the molecular mass of the fuel i in g/mol.

$$W_C' = \frac{W_C}{m_{F,i}} \tag{20}$$

$$W_T' = \frac{W_T}{m_{F,i}} \tag{21}$$

Therefore, the thermal efficiency of the cycle can, also, be obtained considering the work done by the compressor and the turbine per unit of mass of fuel, as shown by Eq. (22).

$$\eta = \frac{W_T' - W_C'}{\frac{n_F\overline{LHV}}{m_{F,i}}} \tag{22}$$

3. RESULTS AND DISCUSSION

Simulations were performed covering the range from 4 to 40 for the compression ratio's value. The work done by the compressor, the work done by the turbine and the thermal efficiency of the constant-pressure combustion thermodynamic cycle and the detonation thermodynamical cycle were analyzed. The results and discussions are presented in the following sub-sections.

3.1 Work done by the compressor

Figure **3** shows the work done by the compressor, in kilojoule per gram of fuel, for the constant-pressure combustion thermodynamic cycle.

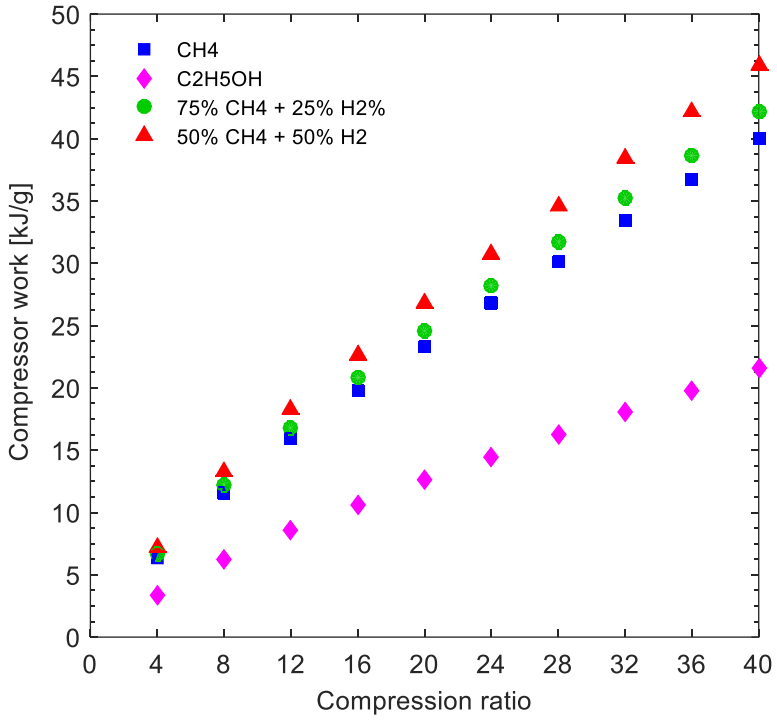

Figure 3. Work done by the compressor in the constant-pressure combustion cycle.

The larger is the compression ratio, the larger is the work performed by the compressor. Figure **3** yields that the work performed by the compressor is slightly similar for methane (CH_4), fuel blend no. 1 ($75\%\ CH_4 + 25\%\ H_2$) and fuel blend no. 2 ($50\%\ CH_4 + 50\%\ H_2$) between compression ratios of 4 and 13. After that point, the compression work remains close for methane and fuel blend no. 1 and, for fuel blend no. 2, it is higher. When the thermodynamic cycle operated with ethanol (C_2H_5OH) as fuel, the work done by the compressor was, in all compression ratios evaluated, lower. Figure **4** shows the work done by the compressor, in kilojoule per gram of fuel, for the detonation thermodynamic cycle.

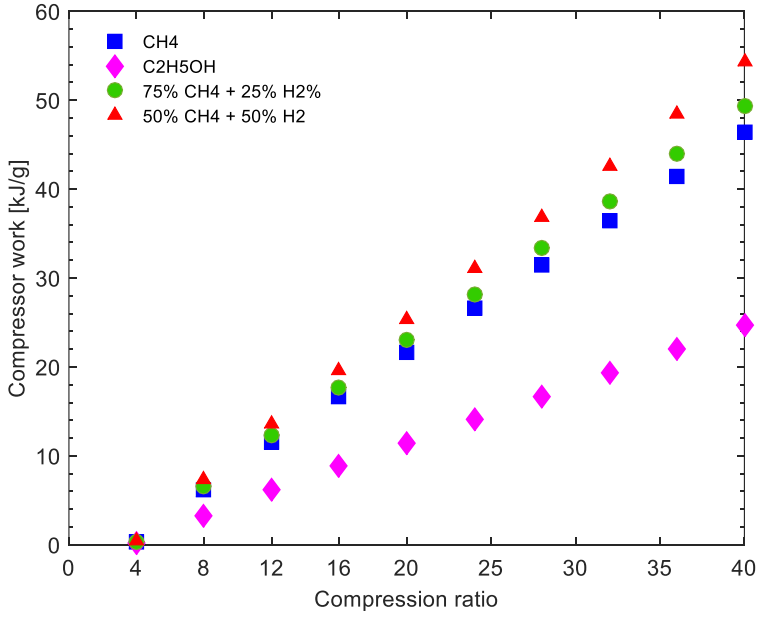

Figure 4. Compression work for the detonation cycle.

The compression work in the detonation cycle performed poorly, for all fuels considered, when the compression ratio is equal to 4. For compression ratios between 8 and 12, the work performed by the compressor is slightly similar for methane (CH_4), fuel blend no. 1 ($75\%\ CH_4 + 25\%\ H_2$) and fuel blend no. 2 ($50\%\ CH_4 + 50\%\ H_2$). For compression ratios higher than 16, the compression work remains close for methane and fuel blend no. 1 and, for fuel blend no. 2, it is higher. For ethanol (C_2H_5OH), the work done by the compressor was, in all compression ratios evaluated, lower. Similar behaviors were observed in the constant-pressure combustion cycle.

3.2 Work done by the turbine

Figure **5** shows the work done by the turbine, in kilojoule per gram of fuel, for the constant-pressure combustion thermodynamic cycle.

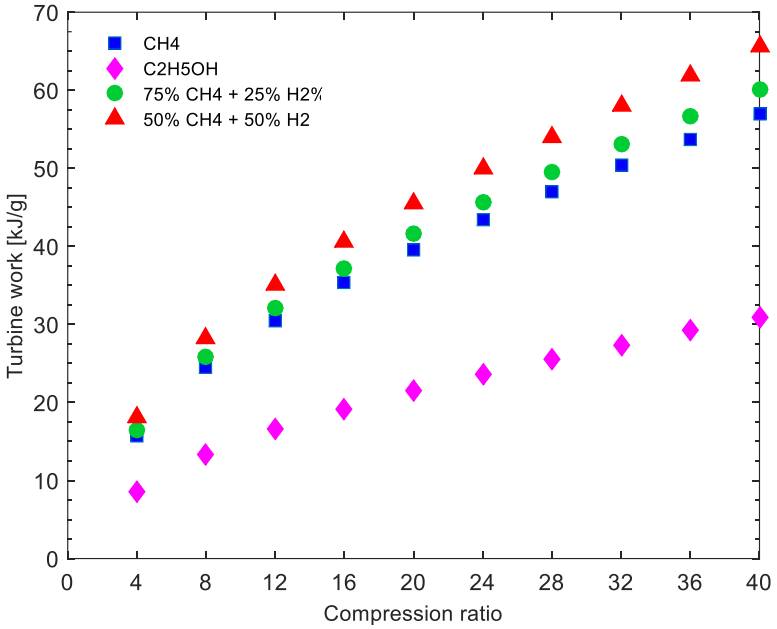

Figure 5. Turbine work in the constant-pressure combustion cycle.

Figure **6** shows the work done by the turbine, in kilojoule per gram of fuel, for the detonation thermodynamic cycle.

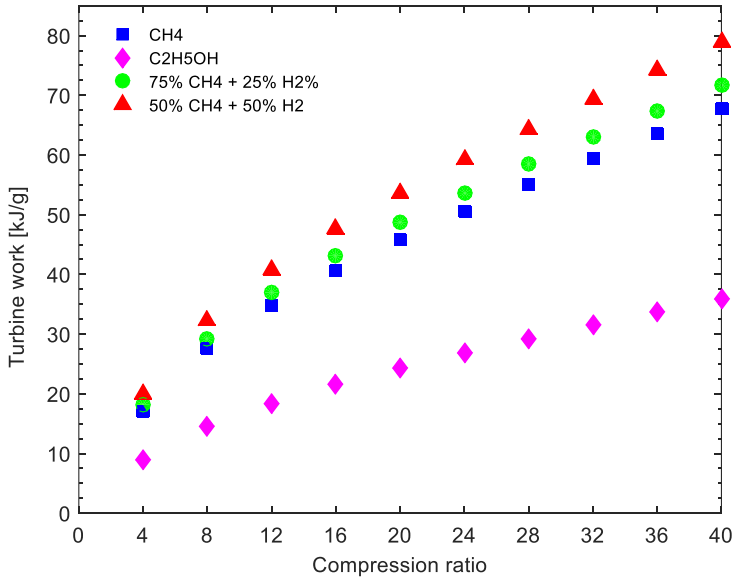

Figure 6. Turbine work in the detonation cycle.

The temperature at the inlet of the turbine and the pressure at the outlet are constant for all cases simulated. The variable parameters, that influence the enthalpy difference between the outlet and inlet of the turbine, are the quantity and composition of the product gases, the quantity of dilution air and the outlet temperature of the air-products mixture.

3.3 Net work

Figure **7** shows the net work performed by the turbine considering the four types of fuel and both thermodynamic cycles. The net work is equal to the turbine work minus the compressor work. On the legend, "c-p.c" stands for "constant-pressure combustion" and "det." stands for "detonation".

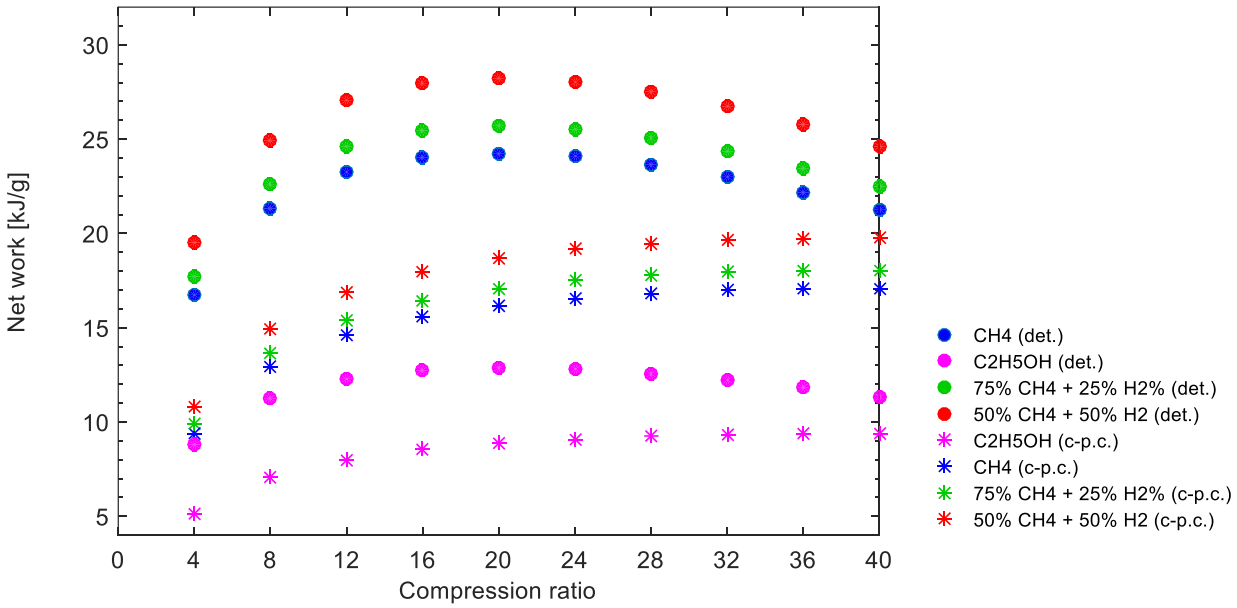

Figure 7. Net work of the turbine.

Comparing each fuel with its respective performance in each cycle, the gas turbine had a higher net work output on the detonation cycle than the constant-pressure combustion net work output. On the detonation cycle, the net work was at its highest when the compression ratio was equal to 20. On the constant-pressure combustion cycle, the larger the compression ratio, the larger is net work output.

3.4 Thermal efficiency

Figure **8** and Figure 9 shows the thermal efficiency of the constant-pressure combustion cycle.

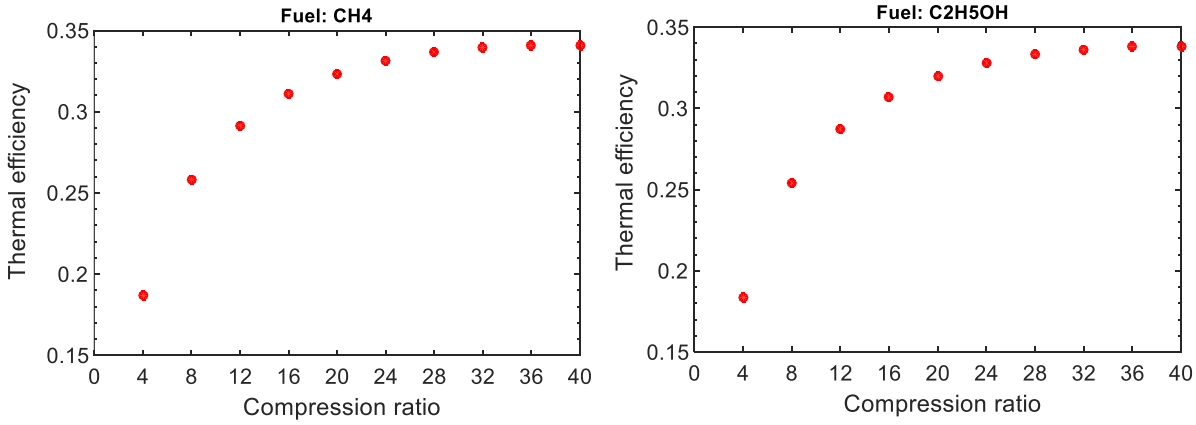

Figure 8. Thermal efficiency of the constant-pressure combustion cycle with CH_4 and C_2H_5OH as fuel.

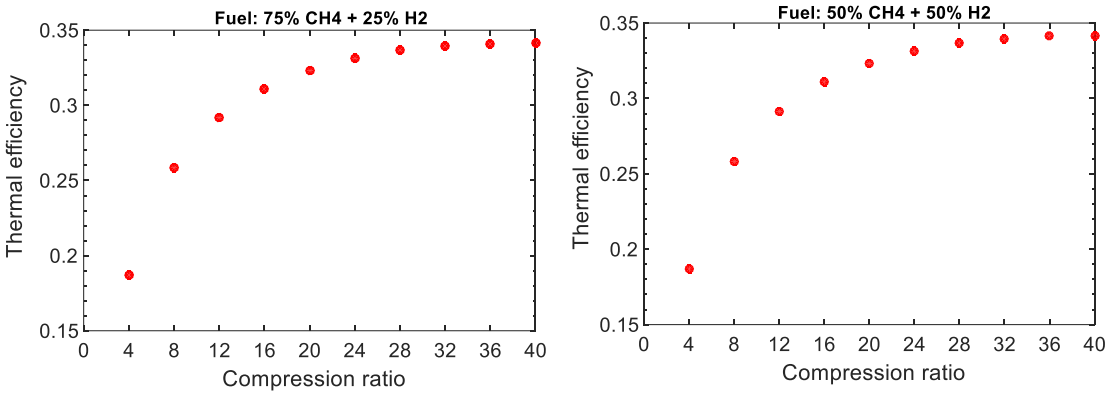

Figure 9. Thermal efficiency of the constant-pressure combustion cycle considering fuel blends no.1 and no.2

The thermal efficiency of the constant-pressure combustion cycle increases as the compression ratio increases. The maximum thermal efficiency was obtained when the compression ratio was at its highest value (40). At this point, an efficiency of 34.10%, 33.84%, 34.12% and 34.15% were obtained for methane, ethanol, fuel blend no. 1 and fuel blend no. 2, respectively. Figure 10 shows the thermal efficiency of the detonation cycle.

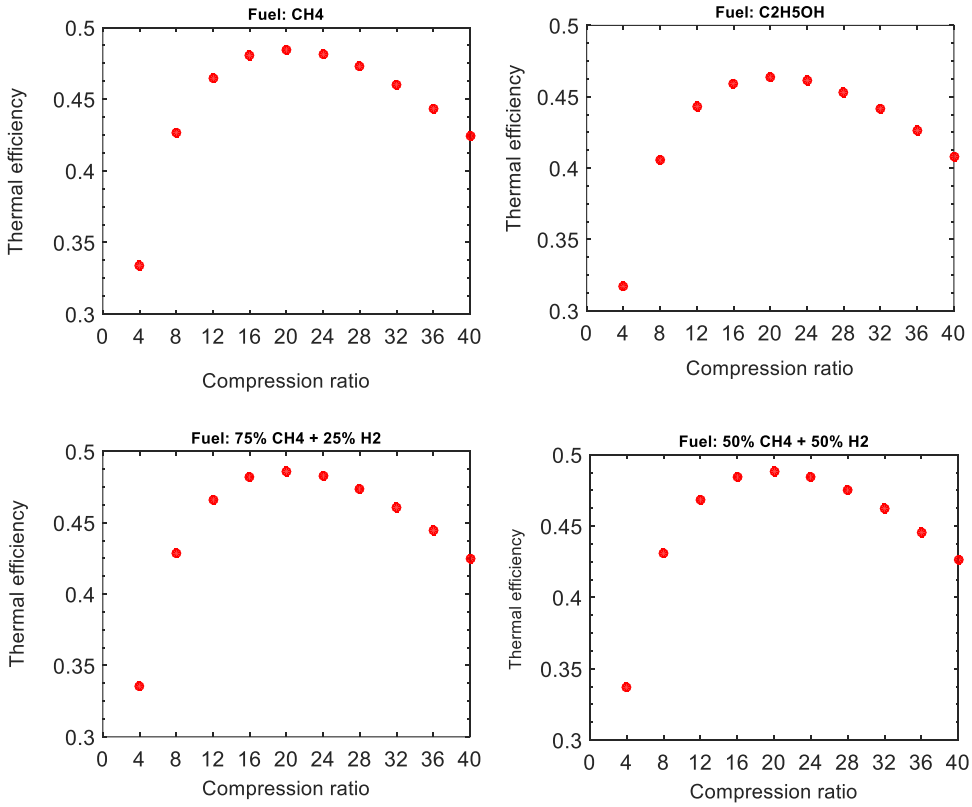

Figure 10. Thermal efficiency of the detonation cycle.

The thermal efficiency of the detonation cycle peaks when the ratio compression equals 20 for all the tested fuels. At this point, an efficiency of 48.47%, 46.39%, 48.6% and 48.81% were obtained for methane, ethanol, fuel blend no. 1 and fuel blend no. 2, respectively.

4. CONCLUSIONS

In the present work Thermodynamic Equilibrium Models for a Constant-pressure Combustion Gas Turbine Cycle and for a Detonation Combustion Gas Turbine Cycle were developed and implemented. The Gibbs Energy Minimization method was applied to determine the species concentrations at the exit of the combustion and detonation chamber,

respectively. Moreover, in the case of the detonation chamber the Chapman – Jouguet theory was also applied to close the system of equations.

Several fuels were considered for the simulations, among them were methane, ethanol, hydrogen and methane – hydrogen mixtures. As expected, the behavior is similar for all fuels. However, the net work was higher for the detonation thermodynamic cycle operating with a mixture of $50\%\ CH_4 + 50\%H_2$ as fuel and a compression ratio equal to 20. In this case, the net work output was, approximately, $28.02\ kJ/g_{fuel}$. Overall, compared to the fuels, ethanol had the poorer performance in each cycle, considering the compressor work, turbine work, net work and thermal efficiency of the cycle.

Compared to the constant-pressure combustion cycle, the detonation cycle possesses a larger thermal efficiency for all fuels at any compression ratio value, and the thermal efficiency of the thermodynamic cycle is maximum when the net work output is maximum. For compression ratios between 4 and 8, the thermal efficiency of the detonation cycle was higher than the constant-pressure combustion thermal efficiency by an average margin of 71%. For compression ranges from 12 to 16, 20 to 24, 28 to 32, and 36 to 40, the increment in thermal efficiency was, respectively, of 56.08%, 46.77%, 37.13% and 26.42%. It is possible that, for compression ratios much greater than 40, the thermal efficiency of the constant-pressure combustion cycle outperforms the efficiency of the detonation cycle. However, this case was not simulated in this paper.

5. ACKNOWLEDGEMENTS

The authors are grateful to CNPq (Conselho Nacional de Desenvolvimento Científico e Tecnológico) for supporting this work through Project 423369/2018-0 and to FAPERGS (Fundação de Apoio à Pesquisa do Estado de Rio Grande do Sul) for supporting this work through Project 21/2551-0000677-3.

6. REFERENCES

Anand, V.; Gutmark, E. “Rotating detonation combustors and their similarities to rocket instabilities”. *Progress in Energy and Combustion Science*, Vol. 73, pp. 182–234. Elsevier BV. [S.L.]

Carvalho Jr., J. A.; Zevallos, A. A. M.; Rodríguez, C. J. C.; McQuay, M. Q., 2018. *Combustão Aplicada*. EdUFSC, Florianópolis, 1st edition.

De Souza, Z., 2014 “Plantas de Geração Térmica a Gás: Turbina a Gás, Turbocompressor, Recuperador de Calor, Câmara de Combustão.” 1st ed. Interciência. Rio de Janeiro, Brazil

Folusiak, M.; Swiderski, K.; Wolanski, P. "Numerical Modeling of the RDE" Transactions on Aerospace Research, Vol. 2020, no .4, 2020, pp.13-47.

Gordon, S.; McBride, B. J.; Zehe, M. J., 2002. “NASA Glenn Coefficients for Calculating Thermodynamic Properties of Individual Species”. NASA. Washington D.C., USA

IUPAC, 1982. “Notation for states and processes, significance of the word standard in chemical thermodynamics, and remarks on commonly tabulated forms of thermodynamic functions.” Pure & Applied Chemistry, Vol. 54, n. 6, pp. 1239–1250. [S.L.]

Kuo, K. K., 2005. *Principles of Combustion*. John Wiley & Sons, Hoboken, 2nd edition.

Lee, J. H. S., 2008. *The Detonation Phenomena*. Cambridge University Press, Cambridge, 1st edition.

Moran M. J.; Shapiro, H. N.; Boettner, D.D.; Bailey, M.B., 2018. *Princípios de termodinâmica para engenharia*. LTC, Rio de Janeiro, 8th edition.

Shapiro, A. H., 1953. *The Dynamics and Thermodynamics of Compressible Fluid Flow*. Ronald Press, New York, Vol 1.

Sousa, J.; Paniagua, G.; Morata, E. C., 2017. “Thermodynamic analysis of a gas turbine engine with a rotating detonation combustor”. Applied Energy. Vol. 195. pp. 247-256.

Wolański, P. “Detonative propulsion”. In *Proceedings of the Combustion Institute*, Vol. 34, n. 1, pp. 125-158, jan. 2013. Elsevier BV. [S.L.]

Xie, Q.; Ji, Z.; Wen, H.; Ren, Z.; Wolański, P.; Wang, B. "Review on the Rotating Detonation Engine and It’s Typical Problems". Transactions on Aerospace Research, Vol. 2020, no .4, 2020, pp.107-163.

Zheng, H.; Qi, L.; Zhao, N.; Li, Z.; Liu, X. 2018. “A Thermodynamic Analysis of the Pressure Gain of Continuously Rotating Detonation Combustor for Gas Turbine”. Applied Sciences, 8, 535.

7. RESPONSIBILITY NOTICE

The authors are the only responsible for the printed material included in this paper.